Some applications of AC impedance spectroscopy in cement research
Gu, P.; Xie, P.; Beaudoin, J. J.

National Research Council Canada   Conseil national de recherches Canada

Canada

Some applications of AC impedance spectroscopy in cement research

NRCC-39840

Gu, P.; Xie, P.; Beaudoin, J.J.

January 1995

National Research Council Canada   Conseil national de recherches Canada

Canada

Ping Gu,[1] Ping Xie,[2] and J J. Beaudoin[1]

Some Applications of AC Impedance Spectroscopy in Cement Research

ABSTRACT: AC impedance techniques have been recently applied to investigate the electrical properties of hydrating cement pastes. A review of recent applications of AC impedance spectroscopy (ACIS) in cementitious materials studies including some relevant applications to microstructural characterization, silica fume content estimation, W-C ratio determination and microcracking of cement paste are presented.

KEYWORDS: AC impedance spectroscopy, cement paste, silica fume, microcracking behavior

The application of AC impedance spectroscopy (ACIS) in cement research is relatively recent although this method has been widely used in electrochemistry (Bonanos et al. 1987). The significance of ACIS for characterizing cement paste systems is dependent on the occurrence of a semicircle in the complex plane at high-frequency range (Fig. 1a). This was first identified for hardened cement paste by McCarter et al. (1988) and McCarter and Brousseau (1990), and studied by Brantervick and Niklasson (1991), Scuderi et al. (1991), Christensen et al. (1992), and the authors (Gu et al. 1992, 1993a, and 1993b). Information related to hydration processes and microstructural development of cement pastes was obtained. These studies indicated that certain parameters obtained from ACIS are very sensitive to microstructural characteristics of cement paste.

Analysis of ACIS uses a simple equivalent electrical circuit model. The corresponding elements are intended to have a clear physical meaning with respect to the microstructure or properties of the system (Xie et al. 1993, Gu et al. 1993c, Xu et al. 1993). A model developed at the National Research Council, Canada reveals that the occurrence of the high-frequency arc results primarily from the presence of solid-liquid interfaces. It can be used to characterize the structural changes in cement-paste systems. A brief review of published work by the authors related to applications of ACIS to microstructural characterization, silica fume content determination, and microcracking of cement paste is presented. The purpose of this review is to introduce and critically evaluate
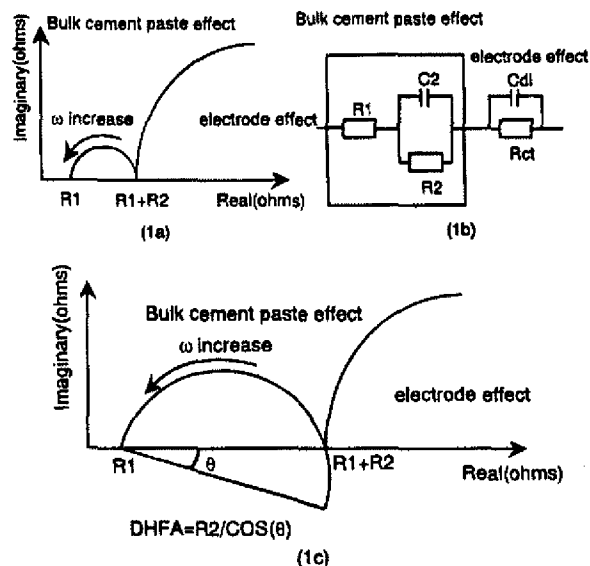
[1]Research associate and principal research officer, respectively, Institute for Research in Construction, Materials Laboratory, Ottawa, Ontario, Canada, K1A 0R6.
[2]Research scientist, University of Ottawa, Department of Civil Engineering, Ottawa, Ontario, Canada, K1N 6N5.

FIG. 1—(a) *Schematic plot of a high-frequency arc in the impedance complex plane obtained for cement paste or concrete systems;* (b) *the corresponding electrical equivalent circuit; and* (c) *an inclined semicircle whose center is depressed below the real axis by an angle* θ.

possible applications of ACIS in cement research; relevant difficulties and limitations will be discussed.

ACIS in Cement Systems

Impedance spectra are generally recorded over a wide range of frequencies from MHz to Hz. A schematic impedance spectrum for a cement paste (two-point measurement configuration) plotted in the real versus imaginary plane (Cole-Cole plot) is illustrated in Fig. 1a. A single arc in the high-frequency range and a small part of a second arc in a relatively low-frequency region are depicted. The high frequency arc (HFA) is attributed to the bulk paste impedance behavior and the second arc is due to the cement paste-electrode surface capacitance. The intercepts R_1 (at the high frequency end) and $R_1 + R_2$ (at the minimum between the electrode arc and bulk arc) are important parameters providing information related to the cement paste and concrete microstructure. The HFA diameter D_{HFA}, is determined from equivalent circuit modeling (Fig. 1b). Ideally, the value of R_2 should be equivalent to D_{HFA} if the HFA is a perfect semicircle. However, an ideal response is rarely observed. Most materials exhibit an inclined semicircle with

the center depressed below the real axis by an angle θ (Fig. 1c). D_{HFA} is then equal to $R_2/\cos(\theta)$.

Impedance spectra for cement paste with $W\text{-}C = 0.35$, at hydration times from 48 to 380 h are plotted in Fig. 2. Only the electrode arc is visible at early hydration times. The HFA appears at a certain time and continues to grow in diameter with hydration time. The detectability of the HFA is dependent on microstructure, ion concentration of pore solution, and equipment limitations (Xie et al. 1994).

Microstructural Characterization of Cement-Based Materials

Previous investigations (Xie et al. 1993, Gu et al. 1993c, Xu et al. 1993) led to the development of the following expressions for the high-frequency resistance (HFR) R_1, and the high-frequency arc diameter D_{HFA} (or R_2):

$$R_1 = \kappa'\left(\frac{1}{1 - \alpha(1 - P)}\right)\left(\frac{1}{\lambda_0(1 - \beta\sqrt{[C]})[C]}\right) \quad (1)$$

and

$$D_{HFA}(\text{or } R_2) = \frac{k_1}{\sigma_f}\left(\delta_{st} + \frac{k_2}{\sqrt{[C]}}\right)\left(\frac{1}{P \cdot r_0}\right) \quad (2)$$

where

κ' = a constant related to cell geometry,
σ_f = ionic conductivity of the interface,
λ_0 = the equivalent conductivity of the pore solution at infinite dilution,
β = an experimental constant associated with ionic interactions and viscosity of the pore solution, and so forth,
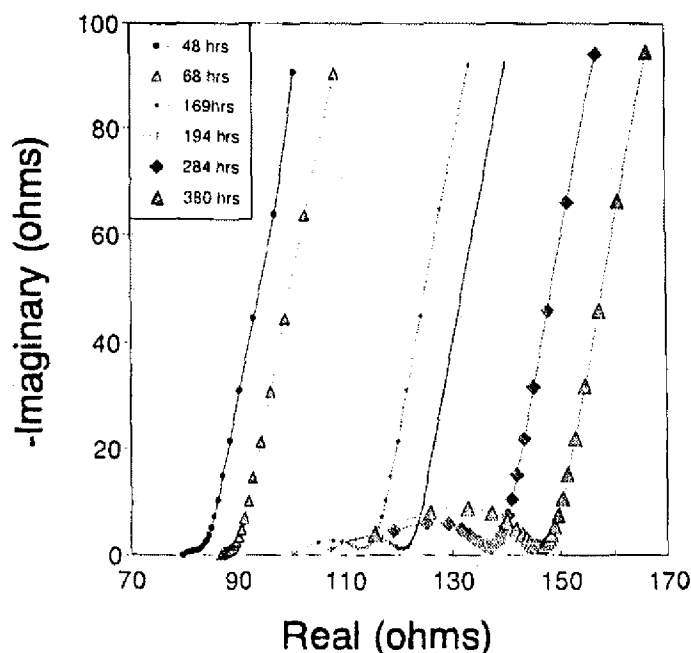
$[C]$ = the concentration of ions in the bulk pore solution,
δ_{st} = the thickness of the Stern layer,
k_1 and k_2 = constants related to pore geometry and ionic strength of pore solution and temperature, respectively,
α = the area fraction-volume fraction ratio of the pores,
P = the pore volume fraction of the cement paste matrix, and
r_0 = mean pore size, determined from a pore-size distribution curve obtained by mercury intrusion porosimetry.

It is noted that (1) R_1 is an inverse function of both pore volume fraction and ionic concentration in the pore solution; (2) D_{HFA} (or R_2) is an inverse function of pore volume fraction, mean pore size, and ionic concentration of the pore solution. The validation of Eqs 1 and 2 were examined by a series of experiments.

R_1 Pore Structure Relationships

A simple relation between the HFR and pore volume is evident from Eq 1. A plot of $1/R_1$ versus P gives a straight line if the concentration term remains relatively unchanged. It may be applicable to hydrated cement systems particularly at advanced hydration times when the conductivity of the pore solution has reached a relatively constant value. Experimental plots of $1/R_1$ versus P for hydrating cement paste systems with $W\text{-}C$ ratios 0.25 and 0.45 are provided in Figs. 3a and 3b, respectively.

D_{HFA} (or R_2) Ionic Concentration of Pore Solution Relationship

The relation between D_{HFA} (or R_2) and the ionic concentration term is examined for mature portland cement pastes immersed in various concentrations of $Na(OH)$ + saturated $Ca(OH)_2$ solution for several hours. It is assumed that the samples are saturated with the solution so that the concentration of $Na(OH)$ may be used to represent the pore solution concentration. A linear relationship between D_{HFA} (or R_2) and $1/[C]^{0.5}$ as described by Eq 2 is illustrated in Fig. 4.

D_{HFA} (or R_2) Pore Structure Relationships

The relationship between D_{HFA} (or R_2) and pore volume fraction as well as pore size distribution of the normal portland cement paste system is demonstrated in Fig. 5. A plot of R_2 versus $1/(P \cdot r_0)$ (r_0 in micrometers) is linear. A correlation coefficient of 0.99 was determined by regression analysis. The pore volume of the specimens varied from 24% at 3 days to 19% at 28 days age and mean pore size ranged from 0.066 to 0.054 μm; $P \cdot r_0$ varied from 0.65 to 0.95.

Determination of Silica Fume Content in Hardened Concrete

Silica fume content in hardened concrete can be obtained from estimates of the high-frequency arc diameter D_{HFA}. The D_{HFA} term reaches a relatively constant value at advanced hydration times because both ionic concentration of the pore solution and the microstructure approach a certain degree of stability. This "final stage" depends on many properties (for example, mineral content and $W\text{-}C$ ratio, and so forth) of the cement paste or concrete. Therefore, ACIS may be used in the determination of those factors

FIG. 2—Real versus imaginary component of impedance of a hydrating cement paste, W-C = 0.35, hydrated from 48 to 380 h.

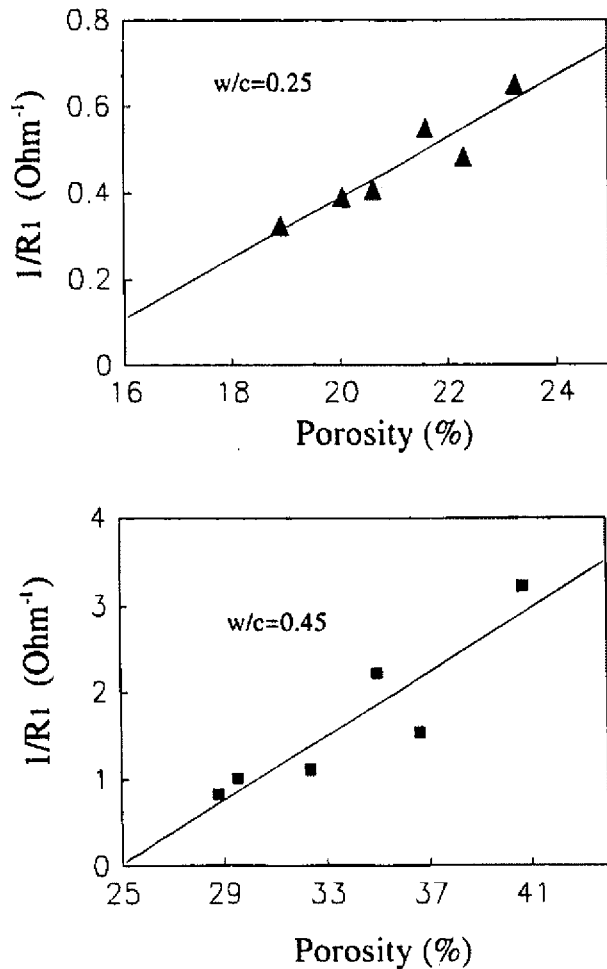FIG. 5—*Plot of* R_2 *versus* $1/P \cdot r_0$ *for ordinary portland cement paste system,* W-C = 0.25.

FIG. 3—*Plots of* $1/R_1$ *versus pore volume fraction for cement paste systems at hydration times from 3 to 27 days with initial* W-C *ratios 0.25 and 0.45.*
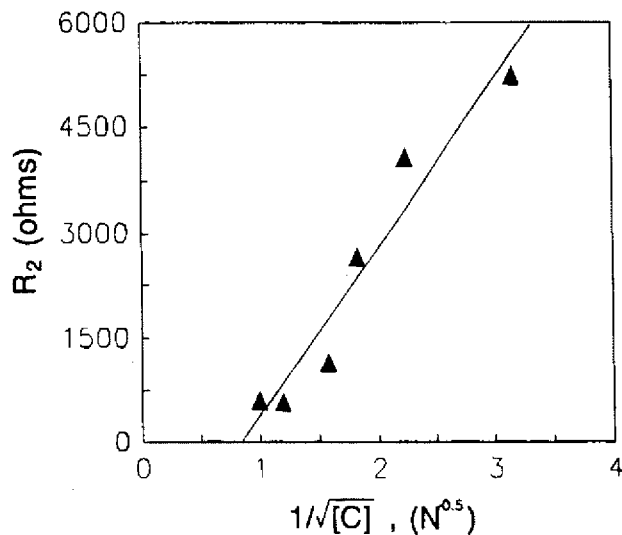

FIG. 4—*Plot of* R_2 *versus* $1/\sqrt{[C]}$, *where* [C] *is the concentration of NaOH in saturated* $Ca(OH)_2$ *solution for mature hardened portland cement pastes.*
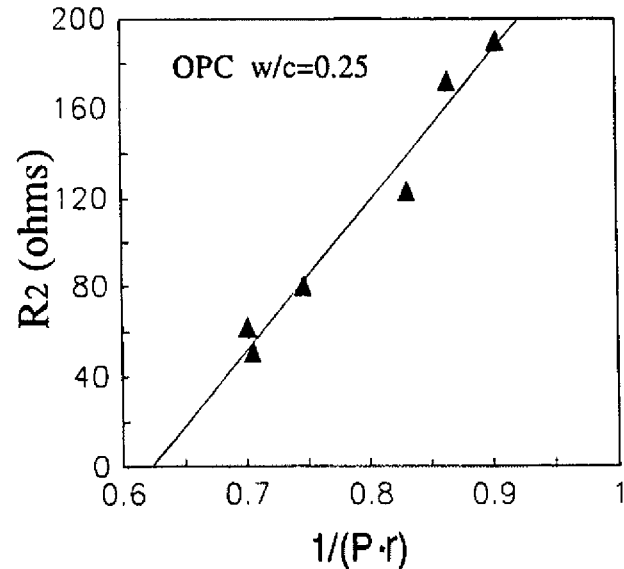
that affect both pore solution conductivity and microstructure, especially at advanced hydration times (assuming the ionic concentration of the pore solution is relatively constant). Plots of D_{HFA} versus silica fume content at advanced hydration times (71 and 81 days) are given in Figs. 6a and 6b. Exponential relations are apparent. The correlation coefficients range from 0.97 to 0.99. The relevant empirical equation has the general form:

$$D_{HFA} = C(K_O)^{\beta_{sf}} \tag{3}$$

or

$$\log D_{HFA} = \log C + \log(K_O)\beta_{sf} \tag{4}$$

where β_{sf} is the silica fume content in percentage, K_O and C are constants related to hydration rate and W-C ratio, and so forth. Straight lines are obtained from plots of $\log D_{HFA}$ versus β_{sf} (Fig. 7).

Determination of W-C Ratio in Hardened Concrete

Water-cement ratio of hardened cement paste can be estimated by ACIS if the pore solution concentration remains relatively constant. A plot of D_{HFA} versus W-C ratio for cement pastes with different initial W-C ratios is provided in Fig. 8. These specimens were immersed in saturated $Ca(OH)_2$ solution for 72 h in order to obtain a similar pore solution concentration condition before the impedance measurements. It is apparent that data obtained at hydration times greater than 6 months lie on a single curve described by an exponential relationship. This is because the change of pore volume is insignificant at advanced ages and similar pore solution concentration. The value of D_{HFA} increases slightly as W-C ratio decreases from 0.8 to 0.4. It increases dramatically as W-C ratio decreases further (ca. 10 times as W-C ratio decreases from 0.80 to 0.25). A threshold appears to occur at about W-C = 0.3. In a conductor (pore solution) insulator (cement hydration products) composite system, the conductivity σ can be described by the percolation equation (McLachlan et al. 1990)
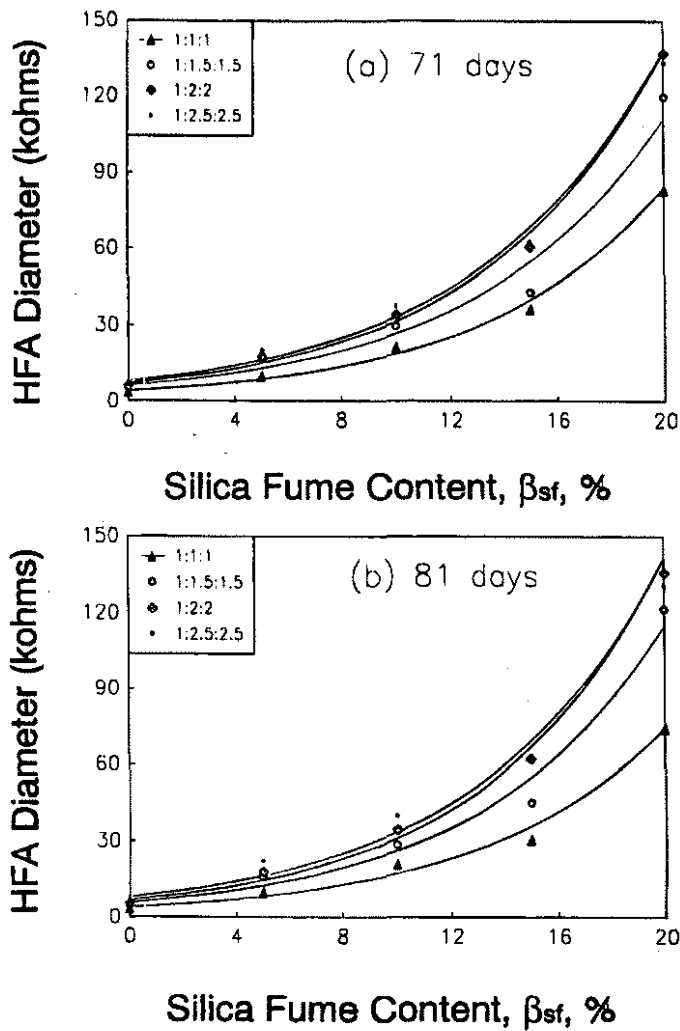
FIG. 6—*Plots of* D_{HFA} *(kΩ) versus silica fume content at advanced hydration times:* (a) 71 (b) 81 days. *The solid lines represent the simulation. Cement-sand-aggregate ratio is indicated.*
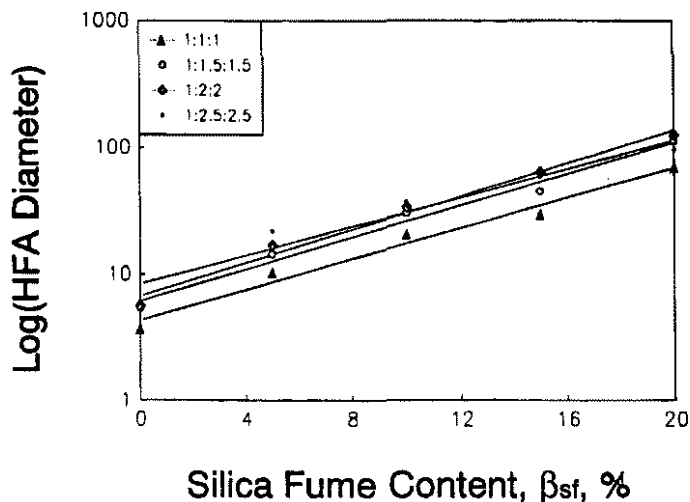

FIG. 7—*A sample plot of* $\log D_{HFA}$ *versus* β_{sf}, *for hydrated concrete containing silica fume at 71 days hydration. Cement-sand-aggregate ratio is indicated.*
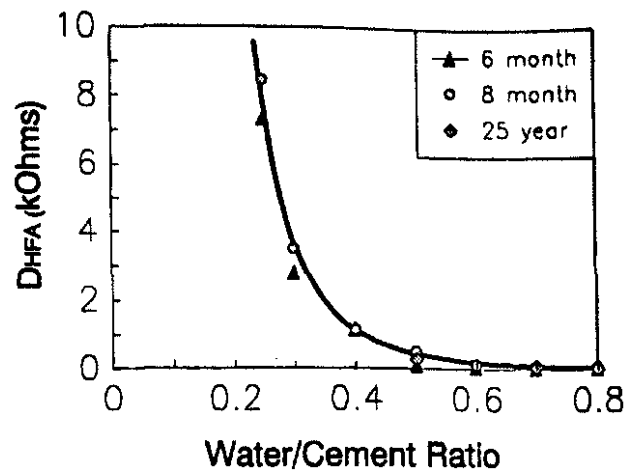

FIG. 8—*A plot of* D_{HFA} *versus* W-C *ratio for cement pastes hydrated 6, 8 months, and 25 years.*

$$\sigma = k\left(\frac{1-f}{f_c}\right)^t \tag{5}$$

where f and f_c are volume fraction and critical volume fraction of the low conductivity phase (cement hydration products), k is a constant, and t is a coefficient related to dispersion of hydration products. The quantity $1-f$ is the liquid phase volume fraction or the pore volume fraction. The original pore volume fraction P_O is simply the volume of water divided by the volume of the water and cement, for example, $P_O = W\text{-}C/W\text{-}C + 0.32$. If it is assumed that $1-f$ is proportional to P_O, Eq 5 can be expressed as follows

$$\sigma = k'\left(\frac{P_O}{f_c}\right)^t \tag{6a}$$

or

$$\log(\sigma) = t \log(P_O) + C \tag{6b}$$

where k' is a constant and $C = \log(k') - t \log(f_c)$. A linear curve
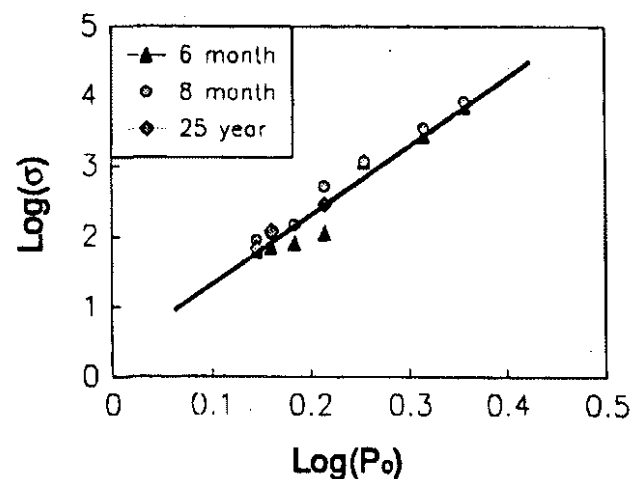

FIG. 9—*Plot of* $\log(\sigma)$ *versus* $\log(P_O)$ *for cement pastes described in Fig. 8.*

is obtained from a plot of $\log(\sigma)$ versus $\log(P_O)$ (Fig. 9), with $t = 9.62$ and $C = 0.52$.

Microcracking in Cement Paste During Compressive Loading

Microstructure of cement paste changes as applied load increases during a compressive test. Changes in microstructure alter the impedance spectrum. Analysis of the impedance behavior therefore may provide information from which inferences of microcrack formation and propagation can be made (Gu et al. 1993d).

D_{HFA} versus applied load P_i curves for pure cement paste and pastes containing 5 and 10% silica fume addition at a hydration time of 15 days are plotted in Fig. 10. The curves contain two distinct regions. Initially, the D_{HFA} decreases slowly with compressive load until a critical point; then its value decreases dramatically until failure takes place.

The normalized data, D_{HFA}/D_{HFAO} versus P_i/P_{im} (the HFA diameters were divided by the initial HFA diameter for example, D_{HFA}/D_{HFAO}, and values of applied loads divided by the maximum load P_i/P_{im}) are given in Fig. 11. The arc diameter ratio decreases slightly for all three D_{HFA}/D_{HFAO} versus P_i/P_{im} curves indicating that microcrack formation may be the controlling process in the initial stage. Dramatic decreases of the diameter ratio may be attributed to subsequent crack propagation. Microcrack propagation becomes large at a load ratio of approximately 0.6 and the decrease of diameter is significant. The microcracking process also

seems to be operative in the cement-silica fume paste systems but large crack propagation occurs at a higher load ratio (that is, 0.9). Addition of silica fume appears to make the initiation of microcracks more difficult. The dramatic decrease of arc diameter reflects the more brittle behavior that results from silica fume addition.

Discussion

The potential of using the ACIS technique in concrete practice is apparent. However, further research is required before this method can be used successfully in field applications. Cement paste is a complex system and its microstructure is randomly formed. The impedance behavior of such a system is determined by both microstructural characteristics and the liquid phase in the pores. It is a difficult challenge to develop ways of determining the conductivity of the liquid phase in-situ in order to accurately determine the in-situ microstructural contribution to impedance.

References

Bonanos, N., Steele, B. C. H., Butler, E. P., Johnson, W. B., Worrell, W. L., MacDonald, D. D., and McKubre, M. C. H., 1987, *Application of Impedance Spectroscopy*, Chapter 4, J. R., McDonald, Ed., Wiley & Sons, NY.

Brantervik, K. and Niklasson, G. A., 1991, "Circuit Models for Cement Based Materials Obtained from Impedance Spectroscopy," *Cement and Concrete Research*, Vol. 21, pp. 469–508.

Christensen, B. J., Mason, T. O., and Jennings, H. M., 1992, "Influence of Silica Fume on the Early Hydration of Portland Cements Using Impedance Spectroscopy," *Journal of the American Ceramic Society*, Vol. 75, No. 4, pp. 939–945.

Gu, P., Xie, P., Beaudoin, J. J., and Brousseau, R., 1992, "A.C. Impedance Spectroscopy (I): A New Equivalent Circuit Model for Hydrated Portland Cement Paste," *Cement and Concrete Research*, Vol. 22, No. 5, pp. 833–840.

Gu, P., Xie, P., Beaudoin, J. J., and Brousseau, R., 1993a, "A.C. Impedance Spectroscopy (II): Microstructural Characterization Hydrating Cement-Silica Fume Systems," *Cement and Concrete Research*, Vol. 23, No. 1, pp. 157–168.

Gu, P., Xie, P., and Beaudoin, J. J., 1993b, "Microstructural Characterization of the Transition Zone in Cement System by Means of A.C. Impedance Spectroscopy," *Cement and Concrete Research*, Vol. 23, No. 3, pp. 581–591.

Gu, P., Xie, P., Xu, Z., and Beaudoin, J. J., 1993c, "Application of A.C. Impedance Techniques in Studies of Porous Cementitious Materials, (I). Influence of Solid Phase and Pore Solution on High Frequency Resistance," *Cement and Concrete Research*, Vol. 23, No. 3, pp. 531–540.

Gu, P., Xu, Z., Xie, P., and Beaudoin, J. J., 1993d, "An A.C. Impedance Spectroscopic Study of Micro-Cracking in Cement-Based Composites during Compressive Loading," *Cement and Concrete Research*, Vol. 23, No. 3, pp. 675–682.

McCarter, W. J., Gearing, S., and Buzzed, N., 1988, "Impedance Measurements on Cement Paste," *Journal of Material Science Letters*, Vol. 7, No. 10, pp. 1056–1057.

McCarter, W. J. and Brousseau, R., 1990, "The A.C. Response of Hardened Cement Paste," *Cement and Concrete Research*, Vol. 20, No. 6, pp. 891–900.

McLachlan, D. S., Blaszkiewicz, M., and Newnham, R. E., 1990, "Electrical Resistivity of Composites," *Journal of the American Ceramic Society*, Vol. 73, No. 8, pp. 2187–2203.
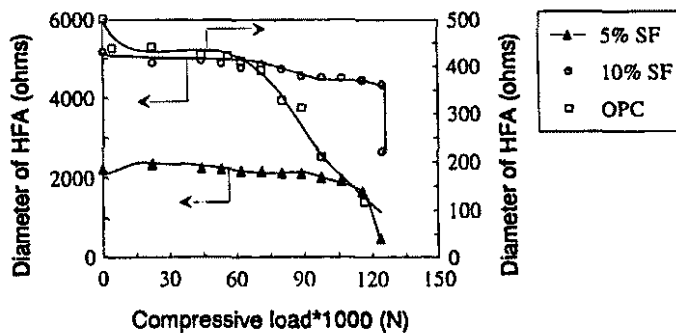
FIG. 10—*Plots of D_{HFA} versus compressive load P_i for pure cement paste and pastes containing 5 and 10% silica fume addition. The W-C ratio is 0.35 and hydration time is 15 days.*
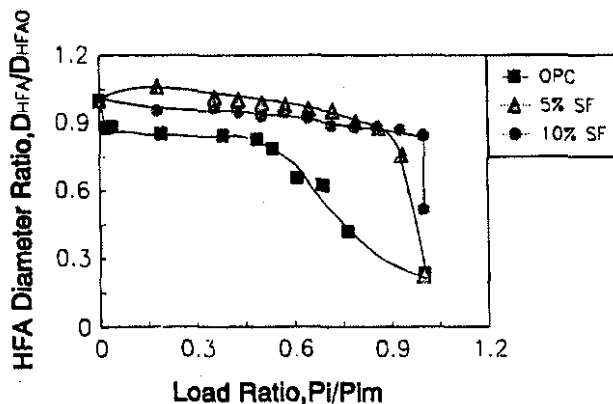

FIG. 11—*Plot of D_{HFA}/D_{HFAO} versus P_i/P_{im} for data shown in Fig. 10.*

Scuderi, C. A., Mason, T. O., and Jennings, H. M., 1991, "Impedance Spectra of Hydrating Cement Pastes," *Journal of Material Science*, Vol. 26, pp. 349–353.

Xie, P., Gu, P., Xu, Z., and Beaudoin, J. J., 1993, "A Rationalized A.C. Impedance Model for Microstructural Characterization of Hydrating Cement Systems," *Cement and Concrete Research*, Vol. 23, No. 2, pp. 359–367.

Xie, P., Gu, P., Fu, Y., and Beaudoin, J. J., 1994, "A.C. Impedance Phenomena in Hydrating Cement Systems: Origin of the High Frequency Arc," *Cement and Concrete Research*, Vol. 24, No. 4, pp. 704–706.

Xu, Z., Gu, P., Xie, P., and Beaudoin, J. J., 1993, "Application of A.C. Impedance Techniques in Studies of Porous Cementitious Materials, (II). Relationship Between ACIS Behavior and the Porous Microstructure," *Cement and Concrete Research*, Vol. 23, No. 4, pp. 853–862.